*J. Chem. Sci.* Vol. 128, No. 7, July 2016, pp. 1149–1155. © Indian Academy of Sciences.
DOI 10.1007/s12039-016-1108-y

# Synthesis and characterization of bi-functional magneto-luminescent $Fe_3O_4@SiO_2@NaLuF_4:Eu^{3+}$ hybrid core/shell nanospheres

JIGMET LADOL[a], HEENA KHAJURIA[a], HAQ NAWAZ SHEIKH[a,*] and YUGAL KHAJURIA[b]
[a]Department of Chemistry, University of Jammu, Jammu 180 006, India
[b]School of Physics, Shri Mata Vaishno Devi University, Katra 182 320, India
e-mail: hnsheikh@rediffmail.com

MS received 15 March 2016; revised 12 April 2016; accepted 2 May 2016

**Abstract.** A step-wise synthetic method has been developed for the synthesis of multifunctional, magnetic luminescent nanocomposites with $Fe_3O_4$ nanospheres as the core encapsulated in silica and europium-doped sodium lutetium fluoride ($NaLuF_4:Eu^{3+}$) as the shell. X-ray powder diffraction (XRPD), scanning electron microscopy (SEM), transmission electron microscopy (TEM), energy dispersive X-ray spectroscopy (EDS), photoluminescence (PL), kinetics of luminescence decay and magnetic studies were used to characterize the structural, optical and magnetic properties of these nanospheres. SEM and TEM images define their spherical morphology with average crystallite size in the range of 90–180 nm. Ultraviolet excited photoluminescent properties of $Eu^{3+}$ doped $Fe_3O_4@SiO_2@NaLuF_4$ nanospheres were investigated and impact of doping has been explored. $Eu^{3+}$ as dopant ion induces highly efficient luminescence with average lifetime value of 6.235 ns. $Fe_3O_4$ magnetic core exhibits super-paramagnetic behavior at room temperature.

**Keywords.** Fluoride; nanostructure; luminescence; magnetic properties; X-ray diffraction.

## 1. Introduction

Multifunctional nanospheres possessing magnetic and fluorescent properties have received increasing attraction in the past decade.[1–4] Super-paramagnetic $Fe_3O_4$ nanospheres, when combined with luminescent lanthanide metal ion gives a wide range of materials for applications including magnetic resonance imaging, drug targets, various medical diagnostics, cancer therapy, recording materials, catalysts and magneto-optic devices.[5–11] Several efforts have been made towards the development of magnetic fluorescent $Fe_3O_4$ nanospheres with large magnetic moment shielded by the lanthanide doped rare-earth metal fluorides/phosphates/oxides. Zhu *et al.*, reported $Fe_3O_4$ nanospheres shielded with $NaLuF_4:Ln^{3+}$ ($Ln^{3+}$ = Yb,Er/Tm) nanospheres.[12] Runowski *et al.*, reported the magnetic and luminescent hybrid nanomaterial based on $Fe_3O_4$ nanocrystals and $GdPO_4:Eu^{3+}$ nano-needles.[13] Multifunctional magneto luminescent nanospheres with $Fe_3O_4$ nanoparticles as the core and $Y_2O_3:Ln^{3+}$ (Ln = Eu; Yb/Er) as the shell were also reported.[14,15] The resulting nanoparticles were observed to exhibit weak fluorescence signal in the absence of silica coating on the surface of $Fe_3O_4$ nanoparticles. This might be due to quenching resulting from energy transfer process between the fluorescent molecules and the metal oxide nanoparticles. Coating of a silica layer on the surface of $Fe_3O_4$ nanospheres plays a significant role in the development of efficient magneto luminescent nanospheres. First, silica layer acting as bridge helps in the successful coating of lanthanide doped rare-earth metal fluorides/oxides shell on iron oxide ($Fe_3O_4$) core. Second, silica being hydrophilic makes the corresponding sample water-soluble. Third, silica inhibits energy transfer process that occurs between lanthanide metal ions and iron oxide core in its absence, thereby reducing the probability of fluorescent quenching. Lanthanide-doped rare-earth fluorides forming the shell are considered as the most efficient host matrices for emission as they possess low phonon energy which decreases the non-radiative relaxation probability and results in more efficient luminescence.[16–18] Among various rare earth fluorides, $NaLuF_4$ proved to be an ideal building block for multimodal bioimaging probes owing to its large atomic number, high luminescence quantum yield and high X-ray absorption coefficient of lutetium.[19–21] Crystal phase also plays an important role on emission properties of $Eu^{3+}$ doped lanthanide fluoride nanocrystals.[22,23] Due to the concerns of toxicity, and optical instability of quantum dots and organic dye molecules used as biomarkers for applications in immunoassay, cell imaging and photodynamic therapy (PDT), lanthanide doped fluorescent nanoparticles have

*For correspondence

become promising alternative materials owing to their superior physical and chemical properties.[24,25]

In this paper, we report the development of a stepwise method for the preparation of multifunctional magnetic-fluorescent nanocomposites with $Fe_3O_4$ nanospheres as the core and $Eu^{3+}$ doped sodium lutetium fluoride ($NaLuF_4$:$Eu^{3+}$) as the shell. Luminescence efficiency of $Eu^{3+}$ doped $NaLaF_4$ nanoparticles present at the surface and super-paramagnetic behavior of $Fe_3O_4$ nanospheres at the core, which are promising for use as luminescent probes in biological labeling and imaging technology, have been studied.

## 2. Experimental

### 2.1 *Materials*

Europium(III) nitrate hexahydrate $Eu(NO_3)_3.6H_2O$ (99.9%), Lutetium(III) nitrate hydrate $Lu(NO_3)_3.H_2O$ (99.9%), Ethylene glycol and sodium fluoride were purchased from Alfa Aesar and used as received without further purification. Ferric chloride hexahydrate $FeCl_3.6H_2O$, tetraethyl orthosilicate (TEOS), trisodium citrate, ethanol, ammonia, sodium acetate and urea were purchased from Himedia Chemical Reagent Company. Deionized water was used throughout.

### 2.2 *Synthesis of $Fe_3O_4$@$SiO_2$@NaLuF4:$Eu^{3+}$ nanospheres*

2.2a *Synthesis of $Fe_3O_4$ nanospheres*: Magnetic $Fe_3O_4$ nanospheres were prepared through a solvothermal reaction. In a typical synthesis, $FeCl_3.6H_2O$ (3.3 mmol, 0.9 g), trisodium citrate (1.3 mmol, 0.38 g), and sodium acetate (18.3 mmol, 1.5 g) were dissolved in ethylene glycol (25 mL) with stirring to form a clear solution. After vigorous stirring at room temperature for about 2 h, colloidal yellow solution was transferred into a 50 mL Teflon-lined autoclave, sealed and heated at 200°C for 12 h. As the autoclave was cooled to room temperature naturally, the black precipitate was separated by centrifugation, washed with deionized water and ethanol three times each.

2.2b *Synthesis of $SiO_2$ coated $Fe_3O_4$ core-shell nanospheres*: The core-shell $Fe_3O_4$@$SiO_2$ nanospheres were prepared by Stober method.[26] The as-prepared $Fe_3O_4$ nanospheres (0.25 mmol, 0.04 g) were dispersed in a solvent mixture containing 70 mL of ethanol, 20 mL of distilled water and 1.5 mL of concentrated ammonia solution. After a time interval of about 15 min, 1 mL of TEOS was added dropwise into the above solution and the solution was kept under stirring for 12 h at room temperature. Synthesized $Fe_3O_4$@$SiO_2$ nanospheres were collected using a magnet and washed several times with water and ethanol in sequence.

2.2c *Synthesis of $Fe_3O_4$@$SiO_2$@$Lu_2O_3$:$Eu^{3+}$ nanospheres*: $Fe_3O_4$@$SiO_2$ nanospheres obtained from the above step were redispersed in 30 mL of distilled water. To this solution, 0.5 mmol of $Ln(NO_3)_3.H_2O$ salt (Ln = Lu and Eu with a molar percentage of 80% $Lu(NO_3)_3$ and 20% $Eu(NO_3)_3$ $.6H_2O$) and 1.5 g urea were added with continuous stirring. The solution was then transferred into a 50 mL Teflon-lined autoclave, sealed and heated at 90°C for 2 h. After cooling, the resultant $Fe_3O_4$@$SiO_2$@Lu, $Eu(OH)CO_3$ precursor was separated with a magnet, thoroughly washed with ethanol and water several times, and further dried at 60°C overnight. Finally, the precursor particles were calcinated at 600°C for 2 h leading to formation of magnetic $Fe_3O_4$@$SiO_2$@$Lu_2O_3$:$Eu^{3+}$ nanospheres.

2.2d *Synthesis of $Fe_3O_4$@$SiO_2$@$NaLuF_4$:$Eu^{3+}$ nanospheres*: 0.02 g of as prepared $Fe_3O_4$@$SiO_2$@$Lu_2O_3$:$Eu^{3+}$ nanospheres was dispersed in a solution (15 mL water) containing 0.14 g of NaF and the mixture was sonicated for 30 min. After sonication, the mixture was sealed in autoclave and heated at 80°C for 2 h. After cooling to room temperature, the resulting $Fe_3O_4$@$SiO_2$@$NaLuF_4$:$Eu^{3+}$ nanospheres were centrifuged and then washed with distilled water several times.

### 2.3 *Spectroscopic and microscopic measurements*

The phase and size of the as-prepared samples were determined from powder X-ray diffraction (PXRD) using D8 X-ray diffractometer (Bruker) at a scanning rate of 12° $min^{-1}$ in the $2\theta$ range from 10° to 70°, with Cu K$\alpha$ radiation ($\lambda$ = 0.15405 nm). Scanning electron microscopy (SEM) analysis of the samples was recorded on FEI Nova NanoSEM 450. High Resolution Transmission Electron Microscopy (HRTEM) was recorded on Tecnai G2 20 S-TWIN Transmission Electron Microscope with a field emission gun operating at 200 kV. Samples for TEM measurements were prepared by evaporating a drop of the colloid onto a carbon-coated copper grid. The energy spectra were obtained by energy-dispersive X-ray spectrum equipped on a Transmission Electron Microscope. The infrared spectrum was recorded on Shimadzu Fourier Transform Infrared Spectrometer (FT-IR) over the range of wave number 4000–400 $cm^{-1}$, and the standard KBr pellet technique was employed. The photoluminescence excitation and emission spectra were recorded at room

temperature using Agilent Cary Eclipse Fluorescence Spectrophotometer equipped with Xenon lamp as the excitation source. Lifetime of luminescent nanospheres was calculated from decay curves using picosecond time-resolved spectrometer, Edinburgh Instruments, Model: FSP920. The magnetic moment as a function of applied field for $Fe_3O_4$@$SiO_2$@$NaLuF_4$:$Eu^{3+}$ was recorded using Vibrating Sample Magnetometer (VSM), Lakeshore 7410. All the measurements were performed at room temperature.

## 3. Results and Discussion

### 3.1 *Crystalline structure and morphology*

The phase and crystallinity of the as-prepared samples were determined using powder X-ray diffraction (PXRD) patterns. The XRPD pattern of $Fe_3O_4$@$SiO_2$@$NaLuF_4$:$Eu^{3+}$ nanospheres (figure 1) confirms the presence of mixture of cubic (JCPDS No. 27-0726) and hexagonal (JCPDS No. 27-0725) phases of $NaLuF_4$ along with some diffraction peaks (marked with stars) of $Fe_3O_4$ phase. The XRPD pattern for $Fe_3O_4$ nanospheres with diffraction peaks at 30.4°, 35.6°, 43.3°, 53.5°, 57.2° and 62.4° corresponding to standard cubic structure of magnetite with JCPDS No. 89-0688 is shown as inset in figure 1.[27] XRPD analysis confirms the successful formation of $NaLuF_4$ phase as shell. $SiO_2$ is not visible in the XRPD pattern because of amorphous nature of silica. Broad diffraction lines indicate that the size of synthesized $Fe_3O_4$@$SiO_2$@$NaLuF_4$:$Eu^{3+}$ nanospheres is in nanoscale.

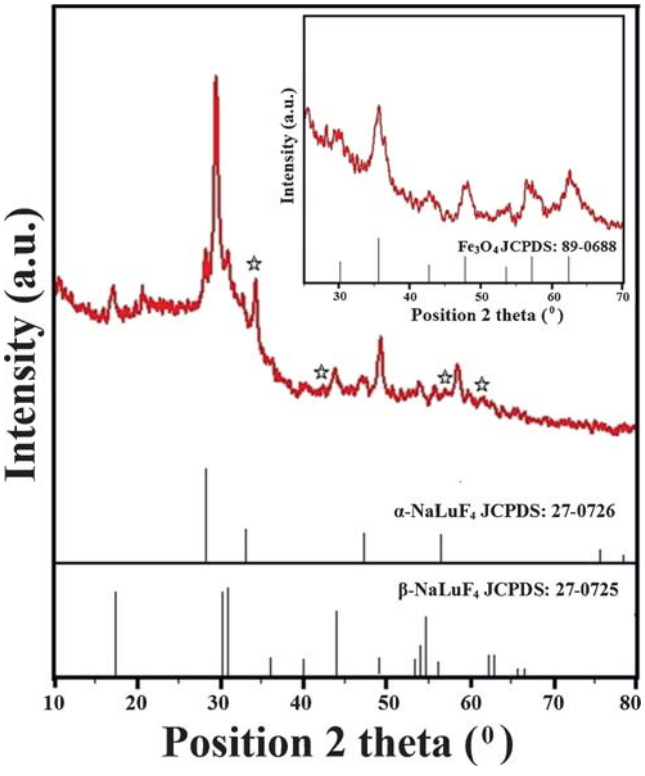


**Figure 1.** XRPD pattern of $Fe_3O_4$@$SiO_2$@$NaLuF_4$:$Eu^{3+}$ core/shell nanospheres. Inset is the XRPD spectrum of $Fe_3O_4$ nanospheres.

The average crystallite size of these nanospheres was calculated according to the Scherrer's equation

$$\beta = \frac{K\lambda}{L\cos\theta} \quad (1)$$

where, L(nm) is the crystallite size, $\lambda$ (nm) is the wavelength of the Cu K$\alpha$ radiant, $\lambda = 0.15405$ nm, $\beta(^\circ)$ is the full-width at half-maximum (fwhm) of the diffraction peak, $\theta$ is the diffraction angle and K is the Scherrer constant equals to 0.89. All the major peaks were used to calculate the average crystallite size of the $Fe_3O_4$ and $Fe_3O_4$@$SiO_2$@$NaLuF_4$:$Eu^{3+}$ core/shell nanospheres. The estimated average crystallite size of $Fe_3O_4$ nanospheres and $Fe_3O_4$@$SiO_2$@$NaLuF_4$:$Eu^{3+}$ core/shell nanospheres are in the range of 80–120 nm and 120–170 nm, respectively, which agree well with TEM image analysis.

The size and morphology of the as-synthesized nanocomposites were characterized using scanning electron microscopy (SEM) and transmission electron microscopy (TEM). SEM images of the $Fe_3O_4$@$SiO_2$ nanospheres, $Fe_3O_4$@$SiO_2$@Lu,Eu(OH)$CO_3$, $Fe_3O_4$@$SiO_2$@$Lu_2O_3$:$Eu^{3+}$ nanospheres and $Fe_3O_4$@$SiO_2$@$NaLuF_4$:$Eu^{3+}$ core/shell nanospheres are shown in figure 2. SEM images confirm the spherical morphology of all the nanospheres synthesized in the step-wise synthetic method.

Figure 3 shows TEM images of nanospheres in sequence of stages involved in the process of formation of $Fe_3O_4$@$SiO_2$@$NaLuF_4$:$Eu^{3+}$ core/shell nanospheres. Figure 3a shows $SiO_2$ coated $Fe_3O_4$ monodispersed nanospheres where dark cores are magnetite nanoparticles and lighter shell surrounding $Fe_3O_4$ cores is amorphous silica. $Fe_3O_4$@$SiO_2$ nanospheres possess smooth surfaces with diameter in the range of 90–120 nm. Further, $Fe_3O_4$@$SiO_2$ nanospheres when coated with lanthanide carbonate layer, Lu,Eu$[(OH)(CO_3)]_2$ are shown in figure 3b. Multilayer $Fe_3O_4$@$SiO_2$@Lu,Eu$[(OH)(CO_3)]_2$ spheres have average diameter of about 330 nm. Multilayer $Fe_3O_4$@$SiO_2$@ Lu,Eu$[(OH)(CO_3)]_2$ spheres when calcined at 600°C for 2 h undergo phase conversion and result in the formation of $Fe_3O_4$@$SiO_2$@$Lu_2O_3$:$Eu^{3+}$ nanospheres are shown in figure 3c. The process of calcination maintained the morphology of $Fe_3O_4$@$SiO_2$@$Lu_2O_3$:$Eu^{3+}$ nanospheres, although the size was reduced from 330 to 180 nm. $Fe_3O_4$@$SiO_2$@$Lu_2O_3$:$Eu^{3+}$ nanospheres were converted into

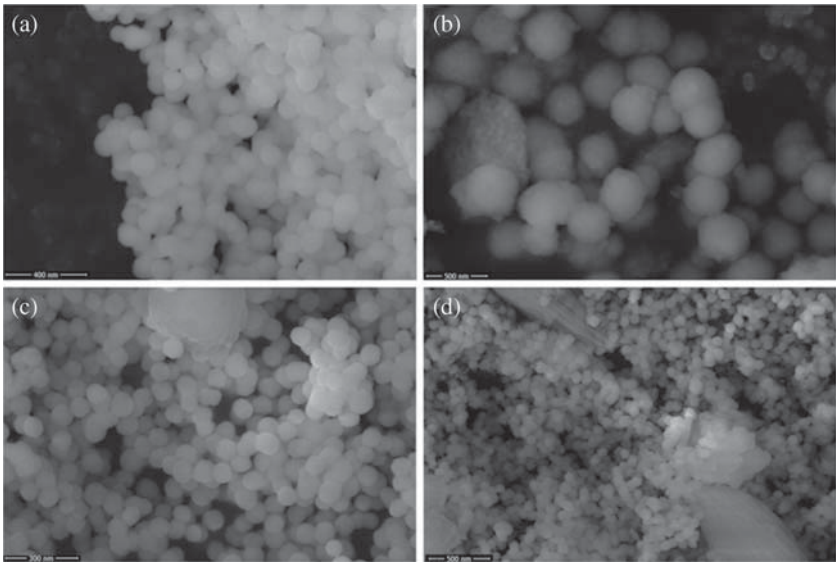


**Figure 2.** SEM images of samples at different step-wise synthetic stages: (a) $Fe_3O_4@SiO_2$, (b) $Fe_3O_4@SiO_2@Lu,Eu(OH)CO_3$, (c) $Fe_3O_4@SiO_2@Lu_2O_3:Eu^{3+}$ and (d) $Fe_3O_4@SiO_2@NaLuF_4:Eu^{3+}$ core/shell nanospheres.

$Fe_3O_4@SiO_2@NaLuF_4:Eu^{3+}$ nanospheres in presence of NaF solution. $Fe_3O_4@SiO_2@NaLuF_4:Eu^{3+}$ nanospheres are also composed of uniform particles with no obvious change in their size but with rough surface as shown in figure 3d. Compositional analysis of $Fe_3O_4@SiO_2$,$Fe_3O_4@SiO_2@$ $Lu,Eu[(OH)(CO_3)]_2$, $Fe_3O_4@SiO_2$

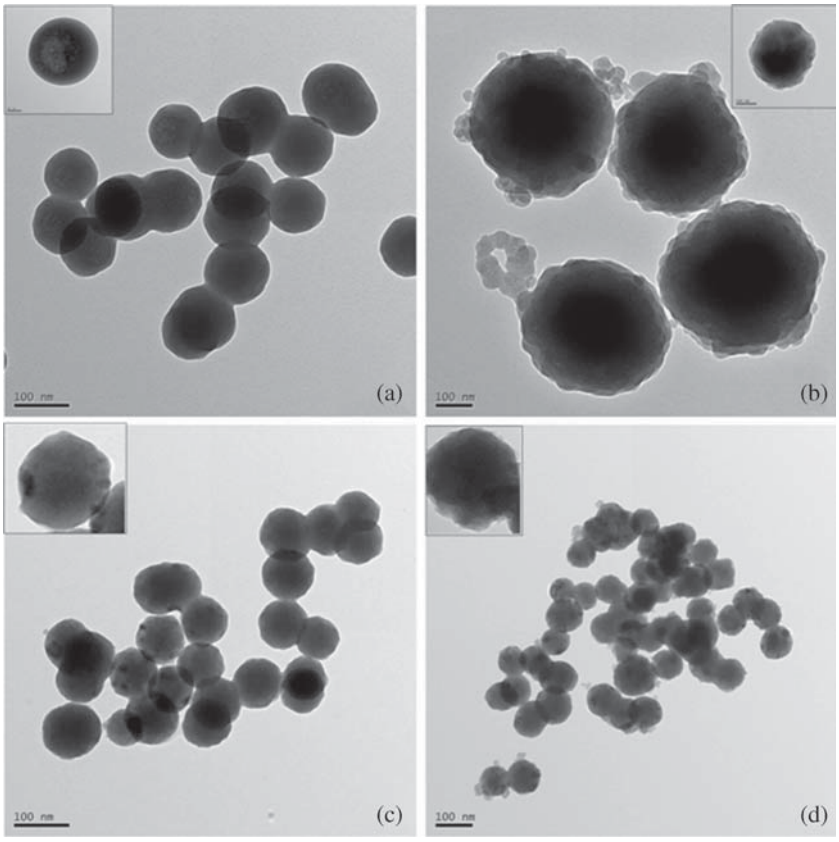


**Figure 3.** TEM images of (a) $Fe_3O_4@SiO_2$, (b) $Fe_3O_4@SiO_2@Lu,Eu(OH)CO_3$, (c) $Fe_3O_4@SiO_2@Lu_2O_3:Eu^{3+}$ and (d) $Fe_3O_4@SiO_2@NaLuF_4:Eu^{3+}$ core/shell nanospheres. Insets are the corresponding images at higher magnification.

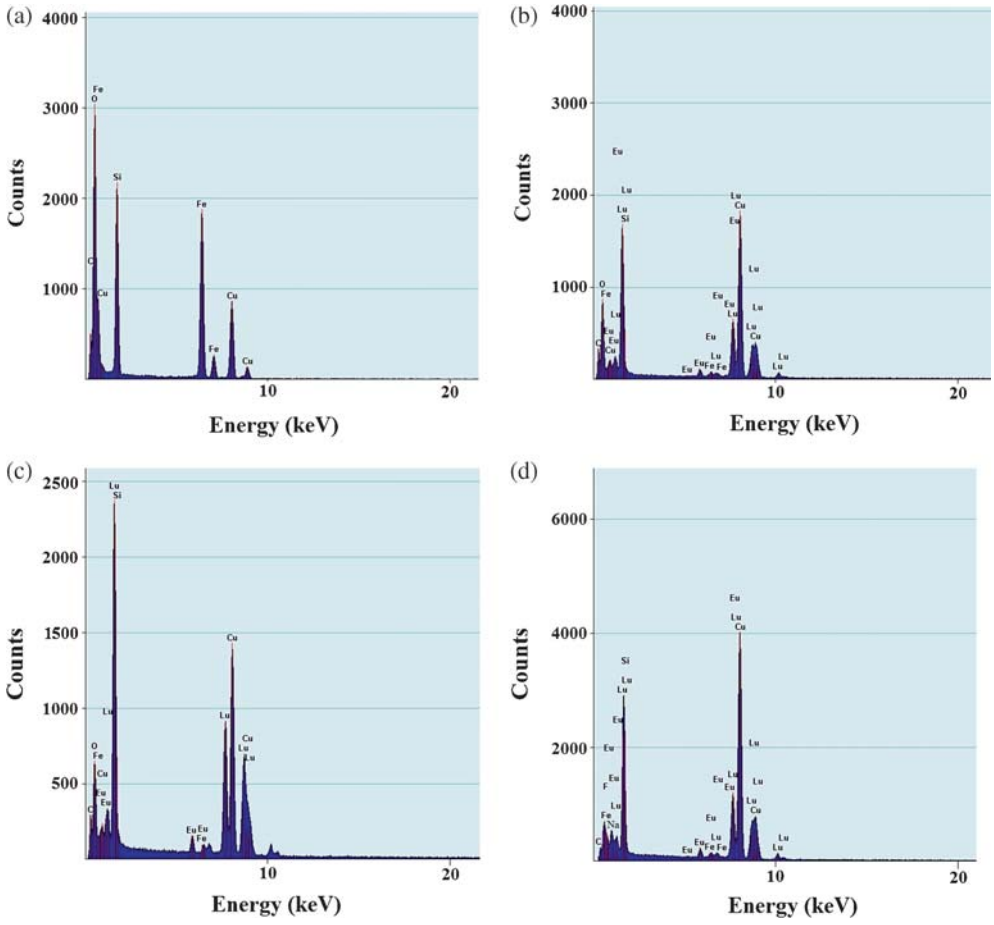


**Figure 4.** EDS spectra of (a) $Fe_3O_4$@$SiO_2$, (b) $Fe_3O_4$@$SiO_2$@Lu,Eu(OH)$CO_3$, (c) $Fe_3O_4$@$SiO_2$@$Lu_2O_3$:$Eu^{3+}$ and (d) $Fe_3O_4$@$SiO_2$@$NaLuF_4$:$Eu^{3+}$ core/shell nanospheres.

@$Lu_2O_3$:$Eu^{3+}$ and $Fe_3O_4$@$SiO_2$@$NaLuF_4$:$Eu^{3+}$ nanospheres were carried out using energy dispersive X-ray spectroscopy (EDS). The EDS spectra and compositional percentage of samples are shown in figures 4a–d and table 1, respectively. The presence of dopant ($Eu^{3+}$) peaks in the EDS spectra suggests successful incorporation of dopant ions in the host lattice. The peaks corresponding to element Na and F in EDS spectra of $Fe_3O_4$@$SiO_2$@$NaLuF_4$:$Eu^{3+}$ nanospheres provide another evidence for the conversion of $Fe_3O_4$@$SiO_2$@$Lu_2O_3$:$Eu^{3+}$ to $Fe_3O_4$@$SiO_2$@$NaLuF_4$:$Eu^{3+}$ nanospheres.

### 3.2 *Ultraviolet excited photoluminescence*

Figure 5a shows the excitation and emission spectra of $Fe_3O_4$@$SiO_2$@$NaLuF_4$:$Eu^{3+}$ core/shell nanospheres measured at room temperature. The excitation spectrum above 350 nm consists of several characteristic excitation lines of $Eu^{3+}$ originating due to the following f–f transitions within the 4f $Eu^{3+}$ ions 317 nm: $^7F_0 \rightarrow {}^5H_6$; 361 nm: $^7F_0 \rightarrow {}^5D_4$; 377 nm: $^7F_0 \rightarrow {}^5G_2$; and 392 nm: $^7F_0 \rightarrow {}^5L_6$. The prominent excitation peak at 392 nm originates from $^7F_0 \rightarrow {}^5L_6$ transition. Excitation

**Table 1.** Atomic and weight % of elements present in prepared samples.

| | $Fe_3O_4$@$SiO_2$ | | $Fe_3O_4$@$SiO_2$@Lu,Eu(OH)$CO_3$ | | $Fe_3O_4$@$SiO_2$@$Lu_2O_3$:$Eu^{3+}$ | | $Fe_3O_4$@$SiO_2$@$NaLuF_4$:$Eu^{3+}$ | |
|---|---|---|---|---|---|---|---|---|
| | At.% | Wt.% | At.% | Wt.% | At.% | Wt.% | At.% | Wt.% |
| C | 38.42 | 16.62 | 33.80 | 14.19 | 35.04 | 15.67 | 34.26 | 14.42 |
| O | 39.46 | 24.34 | 35.19 | 19.69 | 35.55 | 21.18 | 7.79 | 2.98 |
| Si | 10.11 | 11.32 | 2.15 | 2.11 | 4.80 | 5.02 | 20.13 | 13.52 |
| Fe | 0.74 | 0.94 | 0.39 | 0.78 | 0.35 | 0.74 | 0.26 | 0.35 |
| Lu | | | 0.46 | 2.91 | 0.44 | 2.83 | 0.40 | 2.47 |
| Eu | | | 0.11 | 1.63 | 0.10 | 1.44 | 0.12 | 1.55 |
| Na | | | | | | | 12.91 | 4.32 |
| F | | | | | | | 10.03 | 4.55 |

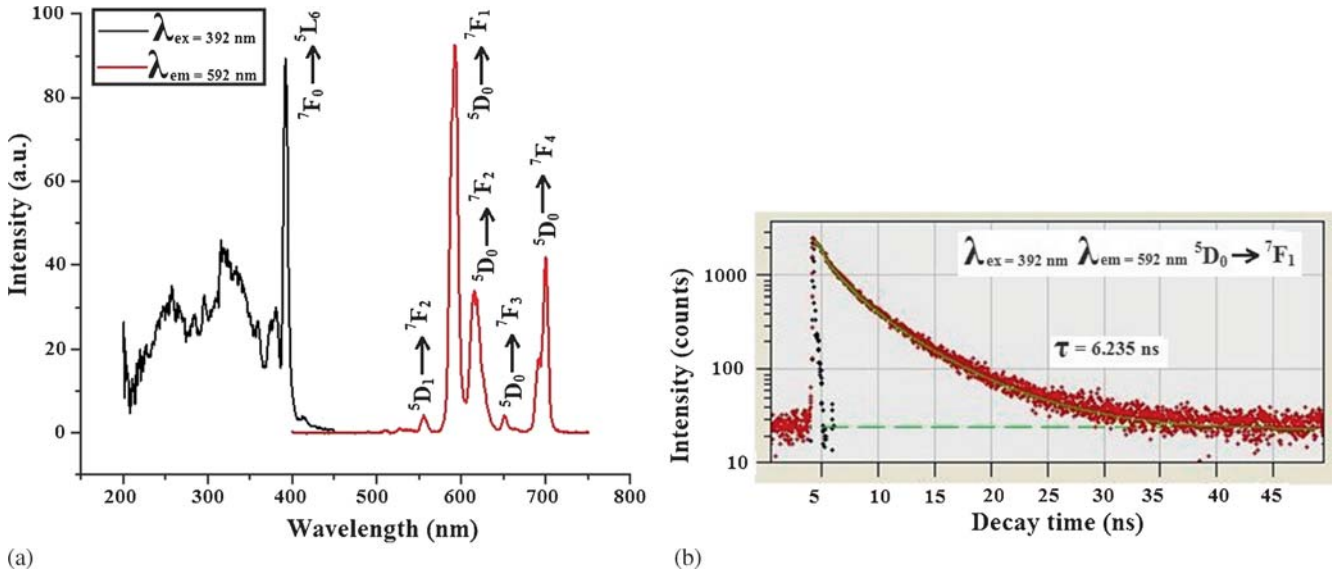


**Figure 5.** Excitation (black) and emission (purple) spectra of, (a) $Fe_3O_4$@$SiO_2$@$NaLuF_4$:$Eu^{3+}$ core/shell nanospheres monitored at $\lambda_{em}$ = 592 nm and $\lambda_{ex}$ = 392 nm; (b) Decay curve of $Eu^{3+}$ luminescence in $Fe_3O_4$@$SiO_2$@$NaLuF_4$:$Eu^{3+}$ core/shell nanospheres.

spectrum in $Fe_3O_4$@$SiO_2$@$NaLuF_4$:$Eu^{3+}$ nanospheres is split more than that of pure $NaLuF_4$:$Eu^{3+}$ nanophosphor.[28] This suggests that the absorption of the UV light by $SiO_2$ shell could influence the excitation spectrum of the prepared material.

The pattern and position of peaks in emission spectrum of synthesized nanospheres are same as that found in pure nanophosphor, $NaLuF_4$:$Eu^{3+}$ reported by Na Niu *et al*.[28] The emission spectrum recorded after exciting the nanospheres at 392 nm consists of prominent emission lines near 556, 592, 615, 651 and 700 nm, which are assigned to characteristic transitions of $Eu^{3+}$ ion $^5D_1 \rightarrow {}^7F_2$, $^5D_0 \rightarrow {}^7F_1$, $^5D_0 \rightarrow {}^7F_2$, $^5D_0 \rightarrow {}^7F_3$ and $^5D_0 \rightarrow {}^7F_4$, respectively. It has been found that if $Eu^{3+}$ is located at inversion centre, the $^5D_0 \rightarrow {}^7F_1$ magnetic dipole transition is dominant, otherwise, the $^5D_0 \rightarrow {}^7F_2$ electric-dipole transition is dominant.[29] In our case, $^5D_0 \rightarrow {}^7F_1$ magnetic-dipole transition is the strongest peak, indicating that the $Eu^{3+}$ ion is located in the $NaLuF_4$ crystal sites with an inversion center. The transitions to the $^7F_{0,3,5}$ levels are forbidden both in magnetic and electric dipole schemes and are usually very weak in the emission spectrum.

The chromaticity coordinates of the $Fe_3O_4$@$SiO_2$@ $NaLuF_4$:$Eu^{3+}$ nanospheres have been calculated from the emission spectrum by using the commission international De I'Eclairage (CIE) system. Figure S1 (in Supplementary Information) shows the CIE chromaticity diagram for $Fe_3O_4$@$SiO_2$@ $NaLuF_4$:$Eu^{3+}$ nanospheres upon excitation at 352 nm. The CIE coordinate is found (0.60, 0.39) for $Eu^{3+}$ doped nanospheres emitting red light. These results indicate very favourable luminescent features of these nanoparticles.

The luminescence decay curve of $Eu^{3+}$ in $Fe_3O_4$@ $SiO_2$@ $NaLuF_4$:$Eu^{3+}$ nanospheres can be well fitted into a single exponential function as $I_{(t)} = I_0 \exp(-t/\tau)$ ($I_0$ is the initial emission intensity at t = 0 and $\tau$ is the lifetime of the emission center). The lifetime of $Eu^{3+}$ in $Fe_3O_4$@$SiO_2$@ $NaLuF_4$:$Eu^{3+}$ nanospheres is 6.235 ns, as shown in figure 5b.

### 3.3 *Magnetic properties*

Besides the efficient UV Photoluminescent property, $Fe_3O_4$@$SiO_2$@$NaLuF_4$:$Eu^{3+}$ nanospheres also exhibit super-paramagnetic behavior at room temperature.

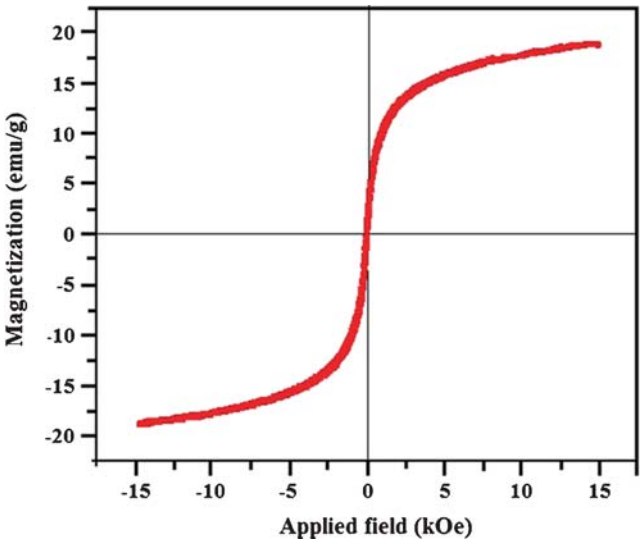


**Figure 6.** Magnetic hysteresis loop measured at 300 K for $Fe_3O_4$@$SiO_2$@$NaLuF_4$:$Eu^{3+}$ core/shell nanospheres.

Measurement of the magnetization as a function of applied field (from −15 kOe to +15 kOe) for $Fe_3O_4$@$SiO_2$@$NaLuF_4$:$Eu^{3+}$ core/shell nanospheres at room temperature is shown in figure 6.

The magnetic hysteresis loop of the magnetic $Fe_3O_4$ @$SiO_2$@$NaLuF_4$:$Eu^{3+}$ core/shell nanospheres demonstrates the classic behavior of super-paramagnetic materials.[30] The coercivity (Hc) of the $Fe_3O_4$@$SiO_2$ @$NaLuF_4$:$Eu^{3+}$ core/shell nanospheres is 23.7 G and the saturation magnetization (Ms) value is about 18.86 emu/g. Superparamagnetic materials are useful for a wide range of applications in biomedicine and biotechnology.[31,32]

## 4. Conclusions

$Fe_3O_4$@$SiO_2$@$NaLuF_4$:$Eu^{3+}$ bifunctional magnetic fluorescence materials were successfully fabricated *via* step-wise synthetic method. The phase and morphology evolution process are well discussed. Photoluminescence studies suggest a general route for the development of highly efficient luminescent down-conversion phosphors which have potential application in diverse fields. Besides highly efficient luminescent phosphors, $Fe_3O_4$@$SiO_2$@$NaLuF_4$:$Eu^{3+}$ core/shell nanospheres also exhibit super-paramagnetic behaviour at room temperature with magnetization of 18.86 emu $g^{-1}$ at 15 kOe. It is expected that these monodispersed bi-functional $Fe_3O_4$@$SiO_2$@$NaLuF_4$:$Eu^{3+}$ core/shell nanospheres with efficient luminescent property and superparamagnetic behavior may have potential applications *in vitro* and *in vivo* dual-modal fluorescent and magnetic bio-imaging and bio-separation. This synthetic procedure is facile, environmentally friendly and may be extended to prepare other materials with submicron disk morphology.

## Supplementary Information (SI)

CIE chromaticity diagram (figure S1) and IR spectrum (figure S2) of $Fe_3O_4$@$SiO_2$@$NaLuF_4$:$Eu^{3+}$ core/shell nanospheres are given in the Supplementary Information, available at www.ias.ac.in/chemsci.

## Acknowledgements

We would like to acknowledge Indian Institute of Technology Mandi and Indian Institute of Technology Guwahati for their technical support. We thank SAIF, Panjab University, Chandigarh for powder X-ray diffraction study and Dr. Vinay Kumar, Assistant Professor, School of Physics, Shri Mata Vaishno Devi University (SMVDU) for photoluminescence studies.

## References

1. Gao J, Zhang B, Gao Y, Pan Y, Zhang X and Xu B 2007 *J. Am. Chem. Soc.* **129** 11928
2. Safari J and Zarnegar Z 2013 *J. Chem. Sci.* **125** 835
3. Yu S Y, Zhang H J, Yu J B, Wang C, Sun L N and Shi W D 2007 *Langmuir* **23** 7836
4. Yu X, Wan J, Shan Y, Chen K and Han X 2009 *Chem. Mater.* **21** 4892
5. Chan Y, Zimmer J P, Stroh M, Steckel J S, Jain R K and Bawendi M G 2004 *Adv. Mater.* **16** 2092
6. Deng Y H, Yang W L, Wang C C and Fu S K 2003 *Adv. Mater.* **15** 1729
7. Maceira S V, Duarte C M A, Spasova M, Marzan L M and Farle M 2006 *Adv. Mater.* **16** 509
8. Meng X, Li H, Chen J, Mei L, Wang K and Li X 2009 *J. Magn. Magn. Mater.* **321** 1155
9. Zi Z, Sun Y, Zhu X, Yang Z, Dai J and Song W 2009 *J. Magn. Magn. Mater.* **321** 1251
10. Phua L X, Xu F, Ma Y G and Ong C K 2009 *Thin Solid Films* **517** 5858
11. Kashevsky B E, Agabekov V E, Kashevsky S B, Kekalo K A, Manina E Y, Prokhorov I V and Ulashchik V S 2008 *Particuology* **6** 322
12. Zhu X, Zhou J, Chen M, Shi M, Feng W and Li F 2012 *Biomaterials* **33** 4618
13. Runowski M, Grzyb T and Lis S 2012 *J. Nanopart. Res.* **14** 1188
14. Ma Z Y, Dosev D, Nichkova M, Gee S J, Hammock B D and Kennedy I M 2009 *J. Mater. Chem.* **19** 4695
15. Yu X, Shan Y, Li G and Chen K 2011 *J. Mater. Chem.* **21** 8104
16. Kramer K W, Biner D, Frei G, Gudel H U, Hehlen M P and Luthi S R 2004 *Chem. Mater.* **16** 1244
17. Kumar G A, Chen C W, Ballato J and Riman R E 2007 *J. Mater. Chem.* **19** 1523
18. Liu C, Wang H, Zang X and Chen D 2009 *J. Mater. Chem.* **19** 489
19. Shi F, Wang J, Zhai X, Zhao D and Qin W 2011 *CrystEngComm.* **13** 3782
20. Niu N, Yang P, He F, Zhang X, Gai S, Li C and Lin J 2012 *J. Mater. Chem.* **22** 10889
21. Zheng K, Liu Z, Lv C and Qin W 2013 *J. Mater. Chem. C* **1** 5502
22. Ghosh P and Patra A 2008 *J. Phys. Chem. C* **112** 19283
23. Ghosh P and Patra A 2008 *J. Phys. Chem. C* **112** 3223
24. Qin X, Yokomori T and Ju Y G 2007 *Appl. Phys. Lett.* **90** 0731041
25. Shan J S and Ju Y G 2007 *Appl. Phys. Lett.* **91** 123103
26. Stober W, Fink A and Bohn E 1968 *J. Colloid. Interface. Sci.* **26** 62
27. Yang T Z, Shen C M and Gao H J 2005 *J. Phys. Chem. B* **109** 23233
28. Niu N, He F, Huang S, Gai S, Zhang X and Yang P 2012 *RSC Adv.* **2** 10337
29. Li C X, Yang J, Yang P P, Lian H Z and Lin J 2008 *Chem. Mater.* **20** 4317
30. Gao J H, Gu H W and Xu B 2009 *Acc. Chem. Res.* **42** 1097
31. Kim J, Piao Y and Hyeon T 2009 *Chem. Soc. Rev.* **2** 372
32. Mulder W J M, Griffioen A W, Strijker G J, Cormode D P, Niolay K and Fayad Z A 2007 *Nanomedicine* **2** 307